Proc. Natl. Acad. Sci. USA
Vol. 88, pp. 1374–1378, February 1991
Biochemistry

In vivo mapping of a DNA adduct at nucleotide resolution: Detection of pyrimidine (6-4) pyrimidone photoproducts by ligation-mediated polymerase chain reaction

(UV photoproducts/photofootprinting/DNA methylation/X-chromosome inactivation)

GERD P. PFEIFER, RÉGEN DROUIN, ARTHUR D. RIGGS, AND GERALD P. HOLMQUIST

Beckman Research Institute of the City of Hope, Department of Biology, Duarte, CA 91010

Communicated by Eugene Roberts, November 6, 1990 (received for review August 29, 1990)

ABSTRACT **DNA adducts in unique sequences along the mammalian genome are mapped *in vivo* at single-nucleotide resolution. Pyrimidine (6-4) pyrimidone photoproducts [(6-4) photoproducts] represent one of the two major adduct classes found after UV irradiation of DNA and were shown to play an important role in UV-induced mutagenesis. After UV light treatment of cells, DNA is prepared and chemically cleaved at (6-4) photoproducts with piperidine. Gene-specific fragments are then amplified from total genomic DNA by use of a ligation-mediated polymerase chain reaction. Analysis of the human chromosome X-linked phosphoglycerate kinase (*PGK1*) gene's promoter has shown that the frequency of (6-4) photoproducts expressed as piperidine-labile sites is (*i*) high at TpC and CpC dinucleotides, (*ii*) dependent on the nearest-neighbor bases, (*iii*) inhibited by the binding of a transcription factor, and (*iv*) different for DNA derived from the active and inactive X chromosome. This latter difference is mainly a consequence of the presence of 5-methylcytosine (m^5C) in CpG dinucleotides on the inactive X chromosome. 5-Methylcytosine in the sequences Tm^5CG and Cm^5CG inhibits the formation of (6-4) photoproducts. Thus, in addition to *in vivo* mapping of a DNA adduct at nucleotide resolution, we also report another method for methylation analysis and photofootprinting.**

Pyrimidine (6-4) pyrimidone photoproducts [(6-4) photoproducts] involve a UV-induced covalent bond between the carbon 6 and carbon 4 of adjacent pyrimidines. Cyclobutane pyrimidine dimers and (6-4) photoproducts (Fig. 1) are the most frequent DNA adducts generated after irradiation of DNA with UV light. Both types of base alterations were shown to be mutagenic in *Escherichia coli* and mammalian cells (refs. 1 and 2; reviewed in refs. 3 and 4) and are implicated in the development of human skin cancer (reviewed in refs. 3 and 5). Whereas cyclobutane dimers have been studied for many years, recognition of (6-4) photoproducts as important UV-induced adducts is more recent. In animal cells, (6-4) photoproducts are more rapidly repaired than cyclobutane pyrimidine dimers (6, 7). Recently, a DNA-binding protein has been detected in UV-irradiated primate cells that is specific for (6-4) photoproducts (8), suggesting that in mammalian cells different pathways may be used for repair of cyclobutane dimers and (6-4) photoproducts (4).

UV damage and repair events have been studied at the single copy gene level in mammalian cells by Southern blot techniques (7, 9). These techniques allow the detection of lesions within restriction fragments by employing adduct-specific endonucleases such as T4 endonuclease V (9) and ABC excinuclease (7, 10). However, more sensitive methods are needed to detect low-frequency strand breaks in single-copy genes at single-nucleotide resolution. Recently, an LMPCR technique was introduced that allows the amplification and detection of DNA fragments that have variable ends on one side and a fixed end on the other side. This technique has been used for *in vivo* footprinting (11, 12), genomic sequencing (13), and determination of strand-specific DNA methylation patterns (12–14). LMPCR is sensitive, allowing the detection of specific bands from as few as 100 molecules of DNA (15). We reasoned that this level of sensitivity should be adequate for the detection of (6-4) photoproducts generated *in vivo*, even though these lesions appear at a frequency of about 10–30% of the frequency of cyclobutane pyrimidine dimers (16, 17).

Here, we show that (6-4) photoproducts can be mapped by LMPCR in irradiated cells at single-copy genes. Using this technique, we have analyzed the distribution of these lesions in a region of the promoter for the phosphoglycerate kinase (*PGK1*) gene on the active and inactive human X chromosome.

MATERIALS AND METHODS

Cell Lines and UV Irradiation. Chinese hamster hybrid cells containing either the active (Y162-11C) or inactive (X8-6T2) human X chromosome (18) were kindly provided by R. S. Hansen and S. M. Gartler (University of Washington, Seattle). Cells were grown to confluent monolayers and irradiated in Petri dishes after removal of the medium. Irradiation was performed using six 254-nm germicidal lamps at a distance of 22 cm. The irradiation times were 30 sec, 60 sec, and 120 sec, corresponding to UV fluxes of 0.6, 1.2, and 2.4 kJ/m^2 as determined by a Blak Ray UV meter (Ultraviolet Products, San Gabriel, CA). For *in vitro* treatments, purified DNA was irradiated in small droplets on Parafilm under the same conditions.

Analysis of (6-4) Photoproducts. Immediately after UV irradiation, cells were trypsinized and DNA was isolated as described (13). Since repair of (6-4) photoproducts requires at least several hours (4), we were isolating unrepaired DNA. DNA was cleaved with *Eco*RI to reduce viscosity, extracted with phenol/chloroform, and precipitated with ethanol. For cleavage at sites of (6-4) photoproducts, DNA was redissolved in 100 μl of 1 M piperidine and heated at 88°C for 30 min. By this treatment, Dewar isomers of (6-4) photoproducts are also cleaved (Fig. 1). The fragments were precipitated in 0.3 M sodium acetate with 2.5 vol of ethanol. After washing in 80% (vol/vol) ethanol, residual traces of piperidine were removed by drying the sample overnight in a Speedvac concentrator. Treatment with 1.2 kJ/m^2 resulted in an average fragment size of about 1500 nucleotides after piperidine cleavage, as determined by alkaline agarose gel electropho-

The publication costs of this article were defrayed in part by page charge payment. This article must therefore be hereby marked "*advertisement*" in accordance with 18 U.S.C. §1734 solely to indicate this fact.

Abbreviations: (6-4) photoproducts, pyrimidine (6-4) pyrimidone photoproducts; LMPCR, ligation-mediated polymerase chain reaction; m^5C, 5-methylcytosine.

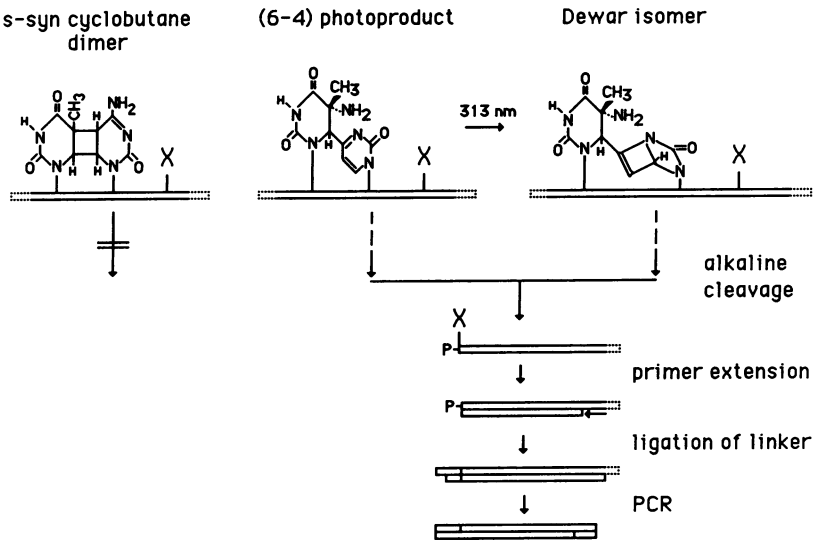

FIG. 1. Outline of (6-4) photoproduct detection by ligation-mediated polymerase chain reaction (LMPCR). Photoproducts of the dinucleotide TpC are shown. X, any DNA base. The open bar below the photoproducts represents the sugar phosphate backbone.

resis. Samples (2–5 μg total DNA) were then processed by LMPCR as described (13). For the Sequenase (Cetus) reactions (primers 1) and PCR amplifications (primers 2) the following primers were used: primer set D (primer D1, 5′-TTTGTCACGTCCGGCAC; primer D2, 5′-ACGCCGCGAACCGCAAGGAACCT; nucleotides −192 to −229); primer set F (primer F1, 5′-CGTCCAGCTTGTCCAGC; primer F2, 5′-TCCAGCGTCAGCTTGTTAGAAAGCG; nucleotides +134 to +99); and primer set J (primer J1, 5′-GCGGTCGGCGCGCTG; primer J2, 5′-CATCGCGGTCGGCGCGCTGCCA; nucleotides −120 to −137). PCR amplification was routinely performed for 19 cycles. The amplified fragments were separated on 8% polyacrylamide sequencing gels, electroblotted onto nylon membranes, and detected by hybridization with a gene-specific single-stranded probe as described (13). A video densitometer (Bio-Rad model 620) together with programs for peak integration (1-D Analyst programs, Bio-Rad) were used for densitometric analysis of the autoradiograms.

RESULTS AND DISCUSSION

(6-4) Photoproducts can be broken at the sites of modified bases by heating in 1 M piperidine (19). Alkali-catalyzed cleavage of irradiated dinucleotides results in products having a 3′-phosphate (20). Accordingly, piperidine treatment of irradiated DNA leads to strand breakage by β-elimination which generates DNA fragments having 3′- and 5′-phosphate groups. Since a 5′-phosphate is present, the fragments obtained after piperidine cleavage are suitable substrates for ligation and can be processed directly for LMPCR (Fig. 1). In this procedure, a gene-specific primer (primer 1) is annealed to the denatured DNA fragments and extended by using Sequenase. This creates blunt-ended double-stranded molecules which then can be ligated to a linker. The introduction of a common linker sequence allows the use of this sequence as a linker-primer together with a second gene-specific primer (primer 2) in a PCR amplification system. After PCR amplification, the DNA fragments are size-fractionated on a sequencing gel, electroblotted onto a nylon membrane, and hybridized with a probe which does not overlap the primer sequences. Dewar isomers (21) are adducts which form from irradiation of (6-4) photoproducts with 313-nm light (22). Since Dewar isomers are extremely alkali labile (23), they are also detected by our LMPCR protocol (Fig. 1). Cyclobutane dimers are not sensitive to alkaline hydrolysis. It is possible to detect cyclobutane pyrimidine dimers at the DNA sequence level by cleavage with a dimer-specific endonuclease (24, 25) which does not cleave (6-4) photoproducts. However, cleavage with this enzyme leaves behind an overhanging pyrimidine dimer at the 5′ end of the damaged strand (24, 26). These fragments did not function as substrates in the LMPCR procedure, unless the overhanging dimer was first split by photolyase (27) treatment (data not shown).

We have investigated the distribution pattern of (6-4) photoproducts expressed as hot-piperidine-labile sites in the promoter region of the human *PGK1* gene. The region was analyzed in Chinese hamster–human hybrid cells which carry an active (cell line Y162-11C) or an inactive human X chromosome (cell line X8-6T2). Figs. 2 and 3 show the analysis of (6-4) photoproducts in the two cell lines at different UV doses. Formation of (6-4) photoproducts is proportional to the UV dose. The background of the procedure (no UV treatment) is relatively low. Some weak bands can be seen in the non-UV-treated samples after prolonged exposure. Most of these correspond to depurination products which are formed by heating in alkali. They do not influence the analysis at sites of pyrimidine photoproducts for which the nonspecific background is very low. Pyrimidine dinucleotides are the major sites of alkali-labile photoproducts, although minor alkali-labile lesions are also detected at some purine bases. The strongest band intensities are seen at several TpC dinucleotides, which is the preferred sequence for formation of (6-4) photoproducts (28). For these sites, we obtained clear signals above background from 80 J/m^2 (not shown); even lower fluences could have produced detectable signal. There are also several CpC sites which form (6-4) photoproducts. The (6-4) photoproduct frequency at CpT and TpT dinucleotides was undetectable (Figs. 2 and 3), consistent with earlier observations (19, 28, 29).

The relative distribution of (6-4) photoproducts was analyzed by densitometry of the individual sequencing lanes. The data are displayed as histograms in Fig. 4. In the LMPCR procedure, band intensities vary from fragment to fragment within a single lane of the sequencing gel (11, 13); this is apparent for the different fragments in the C lane of chemically sequenced DNA (fourth lane in Figs. 2 and 3). Therefore, densitometry was also performed on the control C lanes, and relative band intensities were determined as peak areas for each band in the C lane. The individual bands in the C lanes are derived from approximately equal numbers of molecules, since there is no significant bias of hydrazine

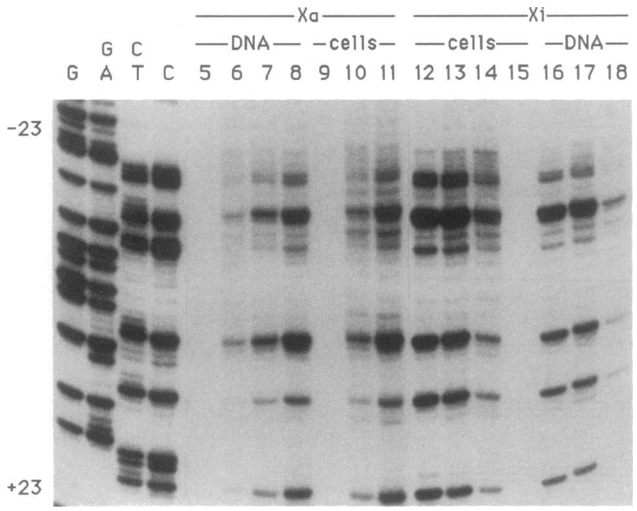

FIG. 2. Determination of (6-4) photoproducts in the promoter region of human *Pgk1*. The region shown (nucleotides −23 to +23) was analyzed with primer set F. It includes the nontranscribed strand near the transcription initiation site. The left four lanes contain products of Maxam–Gilbert sequencing reactions performed on total genomic DNA isolated from HeLa cells. Fragments derived from (6-4) photoproducts comigrate with the position of the 3′ pyrimidine of the dinucleotide when compared with chemically sequenced DNA. Lanes 5–18 show analysis of (6-4) photoproducts in DNA from the active human X chromosome (lanes 5–11) or the inactive human X chromosome (lanes 12–18): lanes 5–8 and 16–18, irradiation of isolated DNA; lanes 9–15, irradiation of intact cells. Lanes 5, 9, and 15 are controls (no UV irradiation). The UV dose was 0.6 kJ/m^2 in lanes 6, 10, 14, and 18; 1.2 kJ/m^2 in lanes 7, 11, 13, and 17; and 2.4 kJ/m^2 in lanes 8, 12, and 16.

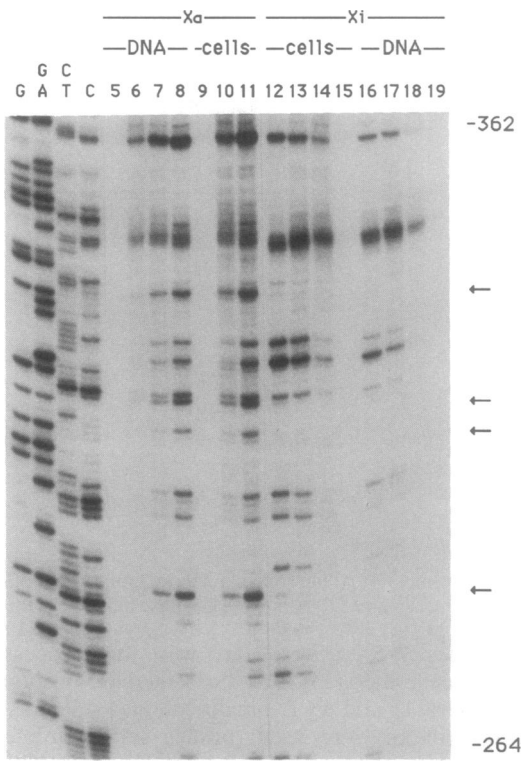

FIG. 3. Determination of (6-4) photoproducts in the 5′ region of human *PGK1*. The region shown was analyzed with primer set D to reveal upper strand sequences from nucleotide −264 to nucleotide −362 relative to the major transcription initiation site. The left four lanes contain products of Maxam–Gilbert sequencing reactions performed on total genomic DNA isolated from HeLa cells. Lanes 5–19 show analysis of (6-4) photoproducts in DNA from the active human X chromosome (lanes 5–11) or the inactive human X chromosome (lanes 12–19): lanes 5–8 and 16–19, irradiation of isolated DNA; lanes 9–15, irradiation of intact cells. Lanes 5, 9, 15, and 19 are controls (no UV irradiation). The UV dose was 0.6 kJ/m^2 in lanes 6, 10, 14, and 18; 1.2 kJ/m^2 in lanes 7, 11, 13, and 17; and 2.4 kJ/m^2 in lanes 8, 12, and 16. Some (6-4) photoproducts which are seen only on the active X chromosome are indicated by arrows.

modification among the different C residues (data not shown). The peak area values determined for sites of (6-4) photoproducts were then divided by the values obtained for the respective band in the C lane. Thus, the numbers given in Fig. 4 have been corrected for the different amplification efficiencies of the individual fragments. The relative frequency of photoproduct formation is different for individual TpC and CpC dinucleotides and depends on the neighboring bases. The strongest signals appear at TpC dinucleotides when a run of several pyrimidines is located 5′ to the TpC. This same rule applies to cyclobutane dimers (28). The sequence TTC always displays a strong TT$^{(6-4)}$C photoproduct. (6-4) Photoproducts at CCC sequences are predominantly formed between the two 5′ cytosines (Fig. 4). In some ACCC sequences, the 5′ cytosine is weakly alkali labile. The chemical nature of this photoproduct is not known, but it could be related to the 2-deoxyribonolactone-containing nucleotides found in ACA sequences after UV irradiation (30).

Since DNA polymerases do not polymerize efficiently across cyclobutane pyrimidine dimers, one might expect that the frequency of (6-4) photoproducts is underestimated when longer DNA fragments are being examined. We have tested this possibility by treatment of irradiated DNA with *E. coli* photolyase (27) prior to piperidine cleavage. The band intensities were found to be slightly (10%) higher for fragments larger than 120 nucleotides and almost identical for smaller fragments. For fragments containing cyclobutane dimer hot spots (e.g., long runs of pyrimidines, A+T-rich DNA) it may be necessary to include the photolyase step.

We have compared the reactivity patterns of DNA derived from the active and inactive human X chromosome (Figs. 2–5). The patterns are overall very similar, with only a few bands having a higher relative frequency at specific sites in DNA from the inactive X chromosome compared with the active X chromosome (Fig. 4). However, there are several (6-4) photoproduct-derived bands which are seen clearly on the active X chromosome but are very weak or absent in DNA from the inactive X chromosome (Figs. 3 and 4). These sites correspond to TpC dinucleotides in the sequence TCG, and CpC dinucleotides in the sequence CCG. A separate genomic sequencing study has shown that the *PGK1* promoter region is unmethylated at every CpG dinucleotide on the active X chromosome in all cell types analyzed (12, 14). In contrast, the same region is methylated at the same sites in DNA from the inactive human X chromosome in X8-6T2 cells. Thus, the difference in reactivity at these sites can be attributed to the differential methylation state of CpG dinucleotides. 5-Methylcytosine (m^{5}C) probably behaves similar to thymine in that TpT and CpT dipyrimidines do not form significant amounts of alkali-labile (6-4) photoproducts (Figs. 2–5). Brash and Haseltine (28) and Glickman *et al.* (31) observed a similar methylation-dependent reduction of (6-4) photoproduct frequency at Cm^{5}CAGG sites in plasmid DNA which was propagated in *E. coli* carrying the *dcm* gene. In this case, the reduction of (6-4) photoproduct formation was correlated with a reduced mutation rate at this site.

The dinucleotide CpG is the most frequent "hot spot" for spontaneous germ-line mutations in the human genome (32). The mutations result from cytosine methylation and a consequent high frequency of spontaneous deamination of 5-methylcytosine to thymine. The predominant mutation attributed to (6-4) photoproducts is also a C → T transition (3).

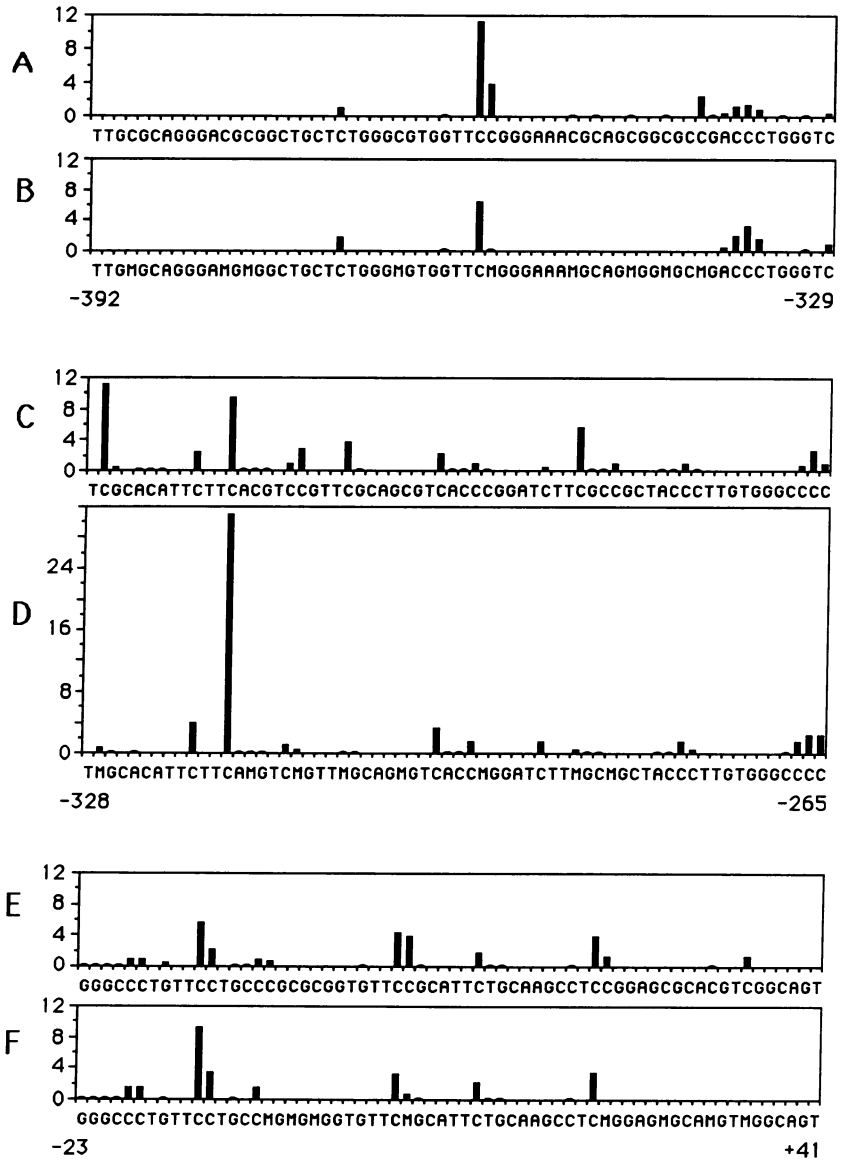

FIG. 4. Summary of the distribution pattern of (6-4) photoproducts expressed as hot-piperidine-labile sites in the human *PGK1* promoter region. Densitometry was performed on samples derived from cells irradiated at 1.2 kJ/m^2 with UV light. The columns represent the relative lesion frequency at a particular base as the percent of total lesions in the whole region analyzed. *A*, *C*, and *E*, the active human X chromosome; *B*, *D*, and *F*, the inactive human X chromosome. M, 5-methylcytosine.

However, in cells exposed to sunlight, cytosine methylation could have the opposite effect on this specific mutation pathway. Since DNA methylation is correlated with gene inactivity (33–35) and inactive regions are more slowly (more inefficiently) repaired than are active regions of the genome (9, 36, 37), the effect of gene activity and DNA methylation on mutation rate is more complex than initially assumed.

The inability of 5-methylcytosine to form alkali-sensitive (6-4) photoproducts may be used in a chemical assay system for DNA cytosine methylation at Cm^{5}CG and Tm^{5}CG sequences, which make up about 50% of all methylated sites in mammalian DNA. Presence of 5-methylcytosine is indicated by a missing band in UV-treated genomic DNA compared with UV-treated unmethylated DNA. Prior to this study, only one methylation assay, the absence of reactivity of the methylated base with hydrazine, has been used for genomic sequencing.

Fig. 5 shows that the *in vivo* chromatin environment can protect DNA bases from photodamage. The region around nucleotide −245 contains a GGGCGG consensus sequence for transcription factor SP1. Previously, the G residues in this sequence were shown, by *in vivo* dimethyl sulfate footprinting, to be protected on the active X chromosome in Y162-11C cells but not protected on the inactive X chromosome in X8-6T2 cells (12). Comparison between naked DNA and DNA that had been irradiated within the normal cellular environment revealed that, in Y162-11C cells, the cytosines on the opposite strand of the SP1 consensus sequence (CCGCCC) are significantly less sensitive to formation of (6-4) photoproducts in the cell compared with their susceptibility in naked DNA (Fig. 5, lanes 12–19). This photofootprint is not seen on the inactive X chromosome in X8-6T2 cells (Fig. 5, lanes 4–11). Comparing naked DNA with DNA that had been irradiated within cells, there were only minor differences for the sequences shown in Figs. 2 and 3. Only one minor *in vivo* protein–DNA contact has been detected in these regions (near nucleotide −300, sequence CGTCA) by *in vivo* footprinting with dimethyl sulfate (12).

Analysis of (6-4) photoproducts may be a generally applicable method for photofootprinting (38) of certain DNA-binding proteins in mammalian cells. Classical footprints are usually interpreted as resulting from a bound protein physi-

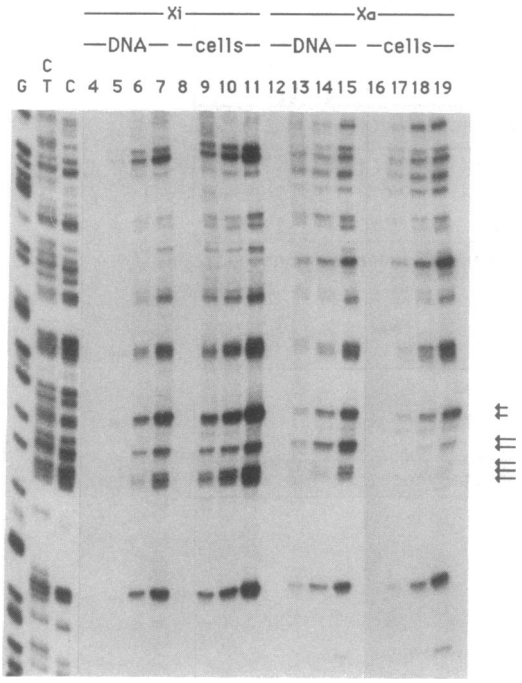

FIG. 5. Photofootprint at the binding site of a transcription factor. Primer set J was used for LMPCR. The region shown (nucleotides −210 to −330, upper strand) contains an SP1 consensus sequence that is protected from UV damage in Y162-11C cells but not in X8-6T2 cells. Protected bases on the active X chromosome are indicated by arrows. The three left lanes contain products of Maxam–Gilbert sequencing controls obtained from HeLa DNA. Lanes 4–19 show analysis of (6-4) photoproducts in DNA from the inactive human X chromosome (lanes 4–11) or the active human X chromosome (lanes 12–19). Irradiation of naked DNA is shown in lanes 4–7 and lanes 12–15, irradiation of cells in lanes 8–11 and 16–19. The UV doses were 0 J/m^2 (lanes 4, 8, 12, 16), 0.6 kJ/m^2 (lanes 5, 9, 13, 17), 1.2 kJ/m^2 (lanes 6, 10, 14, 18), and 2.4 kJ/m^2 (lanes 7, 11, 15, 19).

cally excluding a modifying agent such as DNase from access to the DNA. In contrast, during photofootprinting, a bound protein will absorb only a negligible fraction of the modifying agent, 254-nm light. Therefore, when a pyrimidine base absorbs UV light and is temporarily raised to an excited energy state, we believe the bound protein then directs transition pathways to the ground state which avoid (6-4) photoproduct formation. Becker and Wang (38) more specifically believe that photofootprints are a measure of inflexibility. Since (6-4) photoproduct formation involves a major distortion of the double helix, then photofootprints would represent constrained sequences that cannot attain the required geometry while in the excited state.

We have shown that it is possible to map the frequency of an adduct at single-nucleotide resolution in single-copy genes of mammalian cells. This work may provide the basis for future studies involving the establishment of correlations between DNA damage localization and mutation rates of specific sequences. In addition, it should be possible to investigate DNA repair processes at the DNA sequence level.

We thank G. Sancar for a sample of *E. coli* DNA photolyase and S.-W. Gao for technical assistance. This work was supported by the Beckman Research Institute, by National Institute of Aging Grant AG08196 to A.D.R., and by a fellowship from the Medical Research Council of Canada to R.D.

1. Drobetsky, E. A., Grosovsky, A. J. & Glickman, B. W. (1987) *Proc. Natl. Acad. Sci. USA* **84,** 9103–9107.
2. Bourre, F., Benoit, A. & Sarasin, A. (1989) *J. Virol.* **63,** 4520–4524.
3. Brash, D. E. (1988) *Photochem. Photobiol.* **48,** 59–66.
4. Mitchell, D. L. & Nairn, R. S. (1989) *Photochem. Photobiol.* **49,** 805–819.
5. Friedberg, E. C. (1985) *DNA Repair* (Freeman, New York).
6. Mitchell, D. L. (1988) *Photochem. Photobiol.* **48,** 51–57.
7. Thomas, D. C., Okumoto, D. S., Sancar, A. & Bohr, V. A. (1989) *J. Biol. Chem.* **264,** 18005–18010.
8. Hirschfeld, S., Levine, A. S., Ozata, K. & Protic, M. (1990) *Mol. Cell. Biol.* **10,** 2041–2048.
9. Bohr, V. A., Smith, C. A., Okumoto, D. S. & Hanawalt, P. C. (1985) *Cell* **40,** 359–369.
10. Thomas, D. C., Morton, A. G., Bohr, V. A. & Sancar, A. (1988) *Proc. Natl. Acad. Sci. USA* **85,** 3723–3727.
11. Mueller, P. R. & Wold, B. (1989) *Science* **246,** 780–786.
12. Pfeifer, G. P., Tanguay, R. L., Steigerwald, S. D. & Riggs, A. D. (1990) *Genes Dev.* **4,** 1277–1287.
13. Pfeifer, G. P., Steigerwald, S., Mueller, P. R., Wold, B. & Riggs, A. D. (1989) *Science* **246,** 810–813.
14. Pfeifer, G. P., Steigerwald, S. D., Hansen, R. S., Gartler, S. M. & Riggs, A. D. (1990) *Proc. Natl. Acad. Sci. USA* **87,** 8252–8256.
15. Steigerwald, S. D., Pfeifer, G. P. & Riggs, A. D. (1990) *Nucleic Acids Res.* **18,** 1435–1439.
16. Patrick, M. H. & Rahn, R. O. (1976) in *Photochemistry and Photobiology of Nucleic Acids*, ed. Wang, S. Y. (Academic, New York), Vol. 2, pp. 35–95.
17. Franklin, W. A. & Haseltine, W. A. (1986) *Mutat. Res.* **165,** 1–7.
18. Hansen, R. S., Ellis, N. A. & Gartler, S. M. (1988) *Mol. Cell. Biol.* **8,** 4692–4699.
19. Lippke, J. A., Gordon, L. K., Brash, D. E. & Haseltine, W. A. (1981) *Proc. Natl. Acad. Sci. USA* **78,** 3388–3392.
20. Franklin, W. A., Lo, K. M. & Haseltine, W. A. (1982) *J. Biol. Chem.* **257,** 13535–13543.
21. Taylor, J. S. & Cohrs, M. P. (1987) *J. Am. Chem. Soc.* **109,** 2834–2835.
22. Taylor, J. S., Lu, H. F. & Kotyk, J. J. (1990) *Photochem. Photobiol.* **51,** 161–167.
23. Mitchell, D. L., Brash, D. E. & Nairn, R. S. (1990) *Nucleic Acids Res.* **18,** 963–971.
24. Haseltine, W. A., Gordon, L. K., Lindan, C. P., Grafstrom, R. H., Shaper, L. N. & Grossman, L. (1980) *Nature (London)* **285,** 634–641.
25. Seawell, P. C., Smith, C. A. & Ganesan, A. K. (1980) *J. Virol.* **35,** 790–797.
26. Grossman, L., Caron, P. R., Mazur, S. J. & Oh, E. Y. (1988) *FASEB J.* **2,** 2696–2701.
27. Sancar, A., Smith, F. W. & Sancar, G. B. (1984) *J. Biol. Chem.* **259,** 6028–6032.
28. Brash, D. E. & Haseltine, W. A. (1982) *Nature (London)* **298,** 189–192.
29. Brash, D. E., Seetharam, S., Kraemer, K. H., Seidman, M. M. & Bredberg, A. (1987) *Proc. Natl. Acad. Sci. USA* **84,** 3782–3786.
30. Urata, H., Yamamoto, K., Akagi, M., Hiroaki, H. & Uesugi, S. (1989) *Biochemistry* **28,** 9566–9569.
31. Glickman, B. W., Schaaper, R. M., Haseltine, W. A., Dunn, R. L. & Brash, D. E. (1986) *Proc. Natl. Acad. Sci. USA* **83,** 6945–6949.
32. Cooper, D. N. & Krawczak, M. (1989) *Hum. Genet.* **83,** 181–188.
33. Doerfler, W. (1983) *Annu. Rev. Biochem.* **52,** 93–124.
34. Riggs, A. D. (1989) *Cell Biophys.* **15,** 1–13.
35. Grünwald, S. & Pfeifer, G. P. (1989) *Prog. Clin. Biochem. Med.* **9,** 61–103.
36. Mellon, I., Bohr, V. A., Smith, C. A. & Hanawalt, P. C. (1986) *Proc. Natl. Acad. Sci. USA* **83,** 8878–8882.
37. Ho, L., Bohr, V. A. & Hanawalt, P. C. (1989) *Mol. Cell. Biol.* **9,** 1594–1603.
38. Becker, M. M. & Wang, J. C. (1984) *Nature (London)* **309,** 682–687.